online data

Triosephosphate isomerase deficiency: consequences of an inherited mutation at mRNA, protein and metabolic levels

Judit OLÁH*, Ferenc OROSZ*, László G. PUSKÁS†, László HACKLER, Jr†, Margit HORÁNYI‡, László POLGÁR*, Susan HOLLÁN‡ and Judit OVÁDI*[1]

*Institute of Enzymology, Biological Research Center, Hungarian Academy of Sciences, H-1518, P.O. Box 7, Budapest, Hungary, †Laboratory of Functional Genomics, Biological Research Center, Hungarian Academy of Sciences, H-6701, P.O. Box 521, Szeged, Hungary, and ‡National Institute of Blood Transfusion, Budapest, Hungary

Triosephosphate isomerase (TPI) deficiency is a unique glycolytic enzymopathy coupled with neurodegeneration. Two Hungarian compound heterozygote brothers inherited the same TPI mutations (F240L and E145Stop), but only the younger one suffers from neurodegeneration. In the present study, we determined the kinetic parameters of key glycolytic enzymes including the mutant TPI for rational modelling of erythrocyte glycolysis. We found that a low TPI activity in the mutant cells (lower than predicted from the protein level and specific activity of the purified recombinant enzyme) is coupled with an increase in the activities of glycolytic kinases. The modelling rendered it possible to establish the steady-state flux of the glycolysis and metabolite concentrations, which was not possible experimentally due to the inactivation of the mutant TPI and other enzymes during the pre-steady state. Our results showed that the flux was 2.5-fold higher and the concentration of DHAP (dihydroxyacetone phosphate) and fructose 1,6-bisphosphate increased 40- and 5-fold respectively in the erythrocytes of the patient compared with the control. Although the rapid equilibration of triosephosphates is not achieved, the energy state of the cells is not 'sick' due to the activation of key regulatory enzymes. In lymphocytes of the two brothers, the TPI activity was also lower (20 %) than that of controls; however, the remaining activity was high enough to maintain the rapid equilibration of triosephosphates; consequently, no accumulation of DHAP occurs, as judged by our experimental and computational data. Interestingly, we found significant differences in the mRNA levels of the brothers for TPI and some other, apparently unrelated, proteins. One of them is the prolyl oligopeptidase, the activity decrease of which has been reported in well-characterized neurodegenerative diseases. We found that the peptidase activity of the affected brother was reduced by 30 % compared with that of his neurologically intact brother.

Key words: enzyme deficiency, glycolysis, modelling, neurodegeneration, prolyl oligopeptidase, triosephosphate isomerase.

INTRODUCTION

Triosephosphate isomerase (TPI; EC 5.3.1.1) is a homodimer of two 27 kDa subunits, consisting of 248 amino acids. Three loops of the N-terminal half of the molecule are involved in the intersubunit interaction [1]. The enzyme catalyses the interconversion of D-GAP (D-glyceraldehyde-3-phosphate) and DHAP (dihydroxyacetone phosphate). TPI has been described as a nearly perfect enzyme. The catalysis is a diffusion-controlled process, due to its very high catalytic capacity [2]. TPI deficiency is characterized by haemolytic anaemia and early death in childhood and this is the only glycolytic enzyme defect that is commonly associated with neurodegeneration. The reduced TPI activity results in the elevation of DHAP level by more than an order of magnitude [3–7]. Homozygosity had been reported only for the E104D and V231M mutations. However, several compound heterozygote individuals had been identified, all but one in combination with E104D [4]. Mathematical models have been developed for the glycolytic flux of human erythrocytes [8–10]. These models could achieve good fits with the experimental data in normal cells. However, the model failed to simulate the increase in DHAP concentration measured experimentally in TPI-deficient cells [8,9]. Different explanations were given for this striking discrepancy. All of them were based upon the suggestion that the intracellular TPI activity is significantly lower than predicted from the *in vitro* data. Indeed, the lowering of TPI activity in mutant cells was suggested to be due to the instability of the mutant TPIs [8,9,11] and to its heteroassociation to other cellular components [12]. However, the extremely high DHAP levels could be simulated only by supposing less than 0.1 % of the normal TPI activity [8], which is not supported by experimental data.

In a Hungarian family with TPI deficiency, two germ-line identical, but phenotypically different compound heterozygote brothers inherited two independent mutations, namely F240L and E145Stop, from their mother and from their father respectively [13,14]. The mother and father are symptom-free heterozygotes. The compound heterozygote Hungarian brothers are unique because: (i) only the patient suffers from neurological symptoms, (ii) both of them are beyond 20 years, although all the affected patients described in the literature died at early childhood and (iii) their mutations are distinct from that of other patients. The relative TPI activity of the two brothers is 2–3 %, resulting in 40–60-fold higher DHAP concentration in their erythrocytes as compared with normal controls [15]. Our previous experiments with human recombinant wild-type and mutant (F240L) TPIs have revealed that the specific activity of the recombinant mutant enzyme is 30 % of that of the wild-type isomerase [16]. Phe^{240} is not a direct part of the active site, yet its close proximity to the active site

Abbreviations used: DHAP, dihydroxyacetone phosphate; eNOS, endothelial nitric oxide synthase; FBP, fructose 1,6-bisphosphate; G1,3DP, 1,3-bisphosphoglycerate; G2,3DP, 2,3-bisphosphoglycerate; GAP, glyceraldehyde-3-phosphate; GAPDH, glyceraldehyde-3-phosphate dehydrogenase; HK, hexokinase; PFK, 6-phosphofructokinase; PGM, phosphoglycerate mutase; POP, prolyl oligopeptidase; QRT–PCR, real-time quantitative reverse transcriptase PCR; TPI, triosephosphate isomerase; Z, benzyloxycarbonyl.

[1] To whom correspondence should be addressed (email ovadi@enzim.hu).

and its critical position appear to be essential factors in maintaining the active-site geometry. Our dynamic molecular modelling data suggested that stable heterodimeric TPI consisting of a wild-type or mutant monomer and the truncated fragment (E145Stop) could be formed [17], which is likely to display reduced or no catalytic activity. The formation of the heterodimeric TPI may explain the low TPI activity in the mutation-influenced erythrocytes. The decrease in the TPI level as the possible cause of the reduced TPI activity in the erythrocytes of the two brothers has not been investigated.

Most of the data concerning the TPI deficiency has been obtained with erythrocytes of patients. Erythrocytes are, however, unique cells from several points of view. They have no protein synthesis and DHAP is utilized only by the glycolytic pathway. To obtain information on how relevant the published data are for other cell types and how the mRNA expression, the protein and enzyme activity levels are related to each other, we extended our investigations to lymphocytes. Lymphocytes have been documented to share a couple of similarities with brain cells. These cells share a large number of antigens and receptors. Memory function and storage are similar, and both are characteristic only of these systems [18].

Analysis of mRNA expression and quantitative data for protein and enzyme activity levels in lymphocytes and erythrocytes of the members of the TPI-deficient family are presented with the aim of revealing the consequences of TPI mutations. The mathematical model was evaluated with experimentally determined kinetic parameters to characterize the glycolysis in the deficient cells. Additional factors, which might be involved in the development of neurodegenerative symptoms, were identified at the mRNA level.

MATERIALS AND METHODS

Patients

The clinical and biochemical characteristics of the TPI-deficient Hungarian family have been published previously [15]. Informed consent was obtained from the family members and the age-matched controls.

Materials

ATP, NAD and NADH were purchased from Sigma (St. Louis, MO, U.S.A.). Immobilon-P transfer membrane was purchased from Millipore (Bedford, MA, U.S.A.). All other chemicals were reagent-grade commercial preparations. Milli-Q (Millipore) ultrapure water was used for preparing the solutions.

QRT–PCR (real-time quantitative reverse transcriptase PCR)

QRT–PCR was performed on a RotorGene 3000 instrument (Corbett Research, Sydney, Australia) with gene-specific primers and the SYBR Green method to determine relative mRNA abundance as described in [19]. In brief, 10 μg of total RNA from each sample was reverse transcribed in the presence of poly(dT) sequences in a total volume of 20 μl. After dilution of the mixture with 80 μl of water, 2 μl of this mixture was used as a template in the QRT–PCR. Reactions were performed in a total volume of 20 μl (5 pmol/each forward and reverse primer and 1× ABGene SYBR Green buffer; ABGene, Epsom, Surrey, U.K.) with the following procedure: 10 min at 95 °C, and 45 cycles of 25 s denaturation at 95 °C, 25 s annealing at 60 °C and 20 s extension at 72 °C. Fluorescent signals were gathered after each extension step at 72 °C. Curves were analysed by the RotorGene software (Corbett Research) using dynamic tube and slope correction methods, ignoring data from cycles close to the baseline. Primers were designed by using the ArrayExpress software (Applied Biosystems, Warrington, Cheshire, U.K.). Relative expression ratios were normalized to β-actin and calculated by the method of Pfaffl [20]. All the expression ratios were compared with values obtained from normal individuals. The PCR primers used in the present study are listed in Table 6. Synthetic amplicons were used as standards for calculating absolute mRNA numbers. All the PCRs were performed four times in separate runs with templates from different reverse transcription reactions.

Microarray experiments

Samples and RNA preparation

Total RNAs were isolated from lymphocytes with a NucleoSpin RNA purification kit (Macherey-Nagel, Dürren, Germany) according to the manufacturer's instructions. The quantity and quality of all RNA preparations were assessed by gel electrophoresis and spectrophotometry (NanoDrop; Rockland Technologies, Newport, DE, U.S.A.). Total RNA was used for microarray analysis as well as for QRT–PCR.

Microarray methods

Construction and use of microarrays were performed as described in [21,22]. After printing to Full Moon Biosystems cDNA slides (Full Moon Biosystems, Sunnyvale, CA, U.S.A.), DNA was UV cross-linked to the slides using Stratalinker (700 mJ; Stratagene). Prior to hybridization, the slides were processed as described previously [22,23]. For probe preparation, 2 μg of total RNA was reverse transcribed using the poly-dT primed Genisphere Expression Array 900 Detection system (Genisphere, Hatfield, PA, U.S.A.) in 20 μl total volume using 20 units of RNAsin (Fermentas, Vilnius, Lithuania), 1× first strand buffer (Fermentas) and 200 units of RNase H (−) point mutant M-MLV reverse transcriptase (Fermentas). All the other probe preparation steps were done according to the manufacturer's instructions (Genisphere). Both the first step cDNA hybridization and the second step capture reagent hybridization were carried out in a Ventana hybridization station (Ventana Discovery, Tucson, AZ, U.S.A.) by using the 'antibody' method. First, hybridization was performed at 40 °C for 6 h in 'FGL2' hybridization buffer (10× Denhardt's solution, 0.25 M sodium phosphate buffer, pH 7.0, 1 mM EDTA, 1 × SSC and 0.5 % SDS; where Denhardt's solution is 0.02 % Ficoll 400/0.02 % polyvinylpyrrolidone/0.02 % BSA and SSC is 0.15 M NaCl/0.015 M sodium citrate) and then 2.5 μl of each Cy5 and Cy3 capture reagents were added to the slides in 200 μl of 'Chiphyb' hybridization buffer (Ventana Discovery) and incubated at 42 °C for 2 h. After hybridization, the slides were washed in 0.2 × SSC twice at room temperature (25 °C) for 10 min and then dried and scanned [22]. Scanned output files were analysed using the GenePix Pro6.0 software (Axon Instruments, Foster City, CA, U.S.A.). Each spot was defined by automatic positioning of a grid of circles over the image. For each channel, the median values of feature and the local background pixel intensities were determined [19,22]. The background-corrected expression data were filtered for flagged spots and weak signals. Technical replicates on the same array were averaged. Data were excluded in cases where technical replicates were significantly different. Normalization was performed using the print-tip LOWESS method [24,25]. Genes for which the mean of log ratios across the biological replicates was equal to zero at a significance level $\alpha = 0.05$ are considered to have unchanged expression. On the other hand, genes having a P value smaller than α and the average-fold change (increase or decrease) of the

four data points at least 2.0-fold were considered as regulated genes. All microarray data were formatted following MIAME (minimum information about a microarray experiment) guidelines and were made available in a public database (ArrayExpress; http://www.ebi.ac.uk/arrayexpress/).

Quantitative determination of the amount of TPI

The different haemolysates (with 9 mg/ml haemoglobin content) were equilibrated at room temperature with a suspension of P11 cellulose phosphate cation exchanger in a 10 mM phosphate buffer (pH 6.0) and were centrifuged at 2000 ***g*** for 5 min at 4 °C. The pellets contained the resin-bound proteins, including 99 % of haemoglobin, and a fraction of TPI. The samples were concentrated using an Amicon ultrafiltration stirred-cell apparatus fitted with a YM-3 membrane. The 'lost' TPI amounts were determined by activity measurements in each sample (which was found to be 30–40 % of the total TPI) and used for the determination of the absolute TPI amount. The truncated TPI fragment has no activity; thus its 'loss' during this procedure could not be examined. Aliquots of this haemoglobin-depleted erythrocyte and the lymphocyte lysates were used for SDS/PAGE and immunoblotting. Proteins were electrotransferred on to Immobilon-P transfer membranes. The filters were subjected to immunoblotting with an antiserum directed against rabbit muscle TPI in rat [12]. Antibody binding was revealed by using anti-rat IgG coupled with peroxidase and ECL® (enhanced chemiluminescence) Western Blotting Detection reagents (Amersham Biosciences). TPI amounts were quantified by densitometry using the Bio-Rad Geldoc 1000 densitometer with the Molecular Analyst software (Bio-Rad Laboratories). Calibration was relative to known amounts of rabbit muscle TPI.

Enzyme kinetic measurements

Lysates of erythrocytes and lymphocytes

Packed erythrocytes from control and from members of the TPI-deficient family were prepared as described previously [16].

Protein determination

Routine measurements of protein concentration were by the Bradford method [26]. Haemoglobin concentration was determined spectrophotometrically using an absorption coefficient of 8.77 (414 nm, 0.1 %).

FBP (fructose 1,6-bisphosphate) and DHAP levels in blood

The levels of these glycolytic intermediates were quantified enzymatically as described by Minakami et al. [27].

Activity and flux measurements

The experiments were carried out in a standard buffer (100 mM Tris, pH 8.0) at 37 °C and the NAD–NADH conversion was monitored by a spectrophotometer at 340 nm. Erythrocyte enzyme activities were determined by the method of the International Committee for Standardization in Haematology [28]. GAPDH (glyceraldehyde-3-phosphate dehydrogenase; EC 1.2.1.12) assay was carried out in standard buffer containing 5 mM arsenate, 4 mM NAD and 2 mM GAP as substrates. The conversion of FBP into G1,3DP (1,3-bisphosphoglycerate) was carried out using 5 mM arsenate, 4 mM NAD and 2 mM FBP. POP (prolyl oligopeptidase; EC 3.4.21.26) activity was determined by a fluorimetric assay ($\lambda_{exc} = 340$ nm and $\lambda_{em} = 410$ nm, substrate Z-Gly-Pro-β-naphthylamide; where Z stands for benzyloxycarbonyl) in 100 mM phosphate buffer (pH 8.0) containing 1 mM EDTA and 1 mM dithioerythritol [29].

Determination of changes in DHAP concentration during flux measurements

This method provides an alternative way to follow the conversion of FBP. Since the turbidity of haemolysates does not interfere during the measurement, the amount of haemolysates could be increased 2.5-fold compared with that used for spectrophotometric assays. The reaction mixture contained 5 mM arsenate, 4 mM NAD and 7 mM FBP. The consecutive reactions were stopped at different time points by the addition of ice-cold $HClO_4$ and neutralized as described previously [29a]. The supernatants were used for enzymatic determination of DHAP, applying glycerol-3-phosphate dehydrogenase (EC 1.1.1.8) as auxiliary enzyme [27].

Simulation tools

All the numerical simulations were performed with Mathematica for Students (version 4.2) software package (Wolfram Research; http://www.wolfram.com). V_{max} values of the glycolytic enzymes and all kinetic parameters for the TPI reaction were determined in our system under the same experimental conditions. The rate equations and additional kinetic parameters used for computation of the whole glycolytic pathway were taken from the model of Mulquiney and Kuchel [10] for the glycolytic enzymes. Expressions for bisphosphoglycerate mutase (EC 5.4.2.4), bisphosphoglycerate phosphatase (EC 3.1.3.13) and their parameters were based on the results described in [9]. TPI was assumed to operate via a reversible Michaelis–Menten mechanism. In the model, glycolysis is independent of glucose concentrations, because normally, *in vivo*, erythrocyte glycolysis is always saturated with glucose. Pyruvate, lactate and P_i concentrations were kept constant, because these metabolites can be transported through the cell membrane and the extracellular concentrations are constant.

RESULTS

Relationship between enzyme amount and catalytic activity in erythrocytes

The specific activity of the human recombinant F240L mutant TPI was shown previously to be 30 % of that of the wild-type enzyme [16]. The truncated fragment does not include the active-site residues and, consequently, does not carry activity. Table 1 illustrates that, by assuming wild-type expression levels of the enzyme, the relative TPI activities in the haemolysates of the Hungarian family do not correspond to the activity values predicted by the specific activity of the mutant recombinant enzyme (0.65, 0.50 and 0.15 for the mother, father and the compound heterozygote brothers respectively) [16]. The measured activities in erythrocytes are significantly lower in the mother and the two brothers, but higher in the father.

To establish whether the discrepancy originated from the different protein amounts, the enzyme levels in the erythrocytes for the family members were determined (Figure 1A). The large amount of haemoglobin present in the haemolysates hindered the quantification of TPI amount by Western blotting since the bands of the subunits of haemoglobin and TPI (at 27 kDa) overlap on the SDS/polyacrylamide gel. For this reason, we removed the large part of haemoglobin and quantified the full-length wild-type and/or mutant TPI amount (for details see the Materials and methods section). It has to be noted that the (inactive) truncated fragment could not be detected on the blot, the reason for which is unclear yet. It may be due to the lack of its expression or its fast degradation or to the lack of immunocomplex formation with the polyclonal antisera or to its loss during haemoglobin depletion.

Table 1 mRNA, protein and activity levels of TPI from the members of the Hungarian family determined by QRT–PCR, Western blotting and enzymatic assays respectively

For all determination at least three independent sets of experiments were carried out, and the means ± S.D. are shown. Mutant and truncated TPIs are F240L and E145Stop respectively. The absolute amount of TPI mRNA in lymphocytes was 48 molecules/cell for the control sample. The absolute values of TPI amount and activity in the control haemolysate were 330 μg of TPI/g of haemoglobin and 1900 units/g of haemoglobin; and for the control lymphocyte lysate, these values were 1.75 μg of TPI/mg of protein and 15.0 units/mg of protein respectively.

(a)

Erythrocyte	Composition of alleles (relative activity)	Relative TPI amount	Relative TPI activity
Control	Wild + wild (1 + 1)/2	1	1
Mother	Wild + mutant (1 + 0.3)/2	0.63 ± 0.09	0.42 ± 0.03
Father	Wild + truncated (1 + 0)/2	0.70 ± 0.09	0.67 ± 0.09
Brother	Mutant + truncated (0.3 + 0)/2	0.36 ± 0.05	0.02 ± 0.007
Patient	Mutant + truncated (0.3 + 0)/2	0.44 ± 0.04	0.02 ± 0.007

(b)

Lymphocyte	Composition of alleles	Relative mRNA TPI-2	Relative TPI amount	Relative TPI activity
Control	Wild + wild	1	1	1
Mother	Wild + mutant	2.24 ± 0.92	0.92 ± 0.08	0.72 ± 0.06
Father	Wild + truncated	0.95 ± 0.31	0.65 ± 0.07	0.55 ± 0.05
Brother	Mutant + truncated	0.98 ± 0.11	0.50 ± 0.04	0.22 ± 0.03
Patient	Mutant + truncated	2.24 ± 0.83	0.54 ± 0.04	0.20 ± 0.02

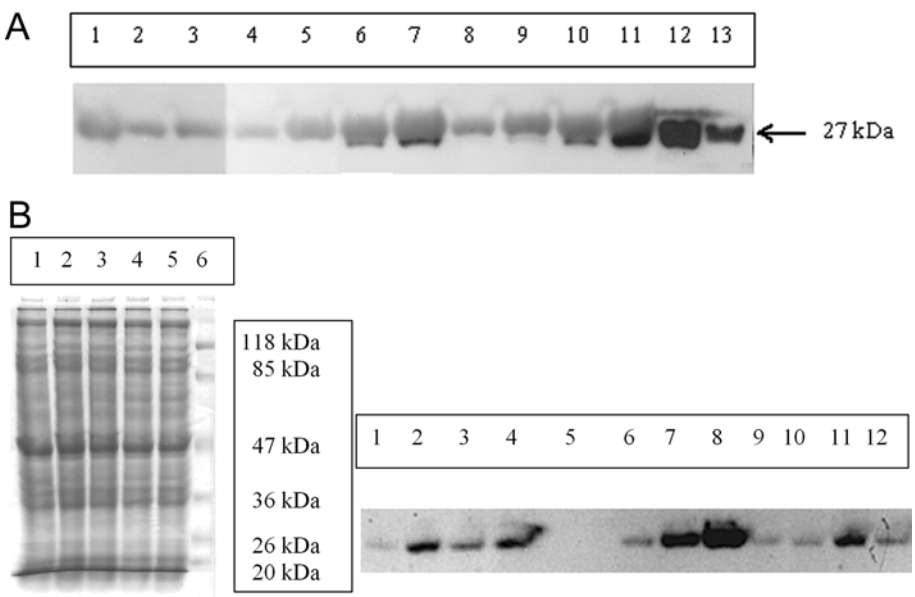

Figure 1 Quantitative determination of TPI level from haemolysates (A) and lymphocytes (B)

(**A**) Western-blot analysis of haemolysates. Lanes 1–3, brother; lanes 4 and 5, patient; lane 6, father; lanes 7–9, mother; lanes 10 and 11, control; lanes 12 and 13, 400 and 100 ng of rabbit muscle TPI. Samples loaded on to the gel contained 0.5 mg of haemoglobin (lanes 2, 4, 8 and 10), 1 mg of haemoglobin (lanes 3, 5, 6, 9 and 11) and 2 mg of haemoglobin (lanes 1 and 7) respectively without haemoglobin depletion. (**B**) SDS/PAGE (left panel) and Western-blot analysis (right panel) of lysates of lymphocytes. Proteins (15 and 40 μg) were loaded in the case of SDS/PAGE and Western blotting respectively. Right panel: lanes 1 and 10, patient; lanes 2 and 11, mother; lanes 3 and 12, father; lane 4, control; lane 5, empty; lanes 6–8, 37, 93 and 186 ng of rabbit muscle TPI; lane 9, brother. Left panel: lane 1, mother; lane 2, father; lane 3, control; lane 4, patient; lane 5, brother; lane 6, molecular mass standard.

The Western-blot data presented in Table 1 show that the amount of full-length TPI is lower in the cases of the mother and the brothers, but it is higher in the father than expected on the basis of the allele compositions (see Table 1). The fact that the enzyme levels are lower only in the cells containing the F240L mutant enzyme (the mother and the two brothers) may suggest that the decrease in the enzyme amount is due to the instability of the missense mutant TPI, which we have reported previously [16].

Table 1 also shows that the TPI activities of the brothers are significantly lower than estimated from the activity decrease caused by the mutation and the expression of the full-length TPI [0.12 relative activity is expected in the case of 0.4 relative enzyme amount (see Table 1)]. The 5-fold lower TPI activity in erythrocytes of the two brothers could be the result of the formation of a heterodimeric species, composed of a mutant monomer and the truncated fragment. The potential formation of such a species was predicted previously in [17].

Consequences of the genetic mutation at the metabolic level

According to our previous results [15] and other reported results [4], the low activity of TPI in the erythrocytes of TPI-deficient patients results in increased DHAP concentration. An inverse relationship between TPI activity and DHAP concentration has

Table 2 Glycolytic enzyme activities in the haemolysates of members of the Hungarian TPI-deficient family

Data are the means for three to five measurements. At least five different sets of experiments were carried out and the means ± S.D. are shown. LDH, lactate dehydrogenase.

	Enzyme activity (units/g of haemoglobin)						
	HK	PFK	Aldolase	TPI	GAPDH	LDH	Pyruvate kinase
Control	0.57–0.67	14.9–19.7	3.6–5.6	1400–2100	100–160	130–190	4.7–6.7
Mother	0.70 ± 0.08	18.6 ± 2.5	5.0 ± 0.6	737 ± 60	150 ± 18	190 ± 10	5.6 ± 0.7
Father	0.70 ± 0.07	20.1 ± 3.0	5.0 ± 0.6	1180 ± 165	145 ± 20	164 ± 20	5.0 ± 0.5
Brother	1.30 ± 0.18	33.4 ± 5.0	6.7 ± 1.5	44.0 ± 14.5	239 ± 22	222 ± 16	9.4 ± 0.8
Patient	1.47 ± 0.22	34.3 ± 5.0	6.7 ± 1.3	36.5 ± 12.5	214 ± 21	159 ± 10	9.9 ± 1.1

been detected for TPI-deficient patients. However, the low TPI activity-derived DHAP accumulation has not been supported by the previous models unless an unrealistically low TPI activity was introduced [8,9].

Our objective was to elaborate a realistic model of human erythrocyte glycolysis on the basis of kinetic parameters determined experimentally in our system. The steady-state flux of the glycolysis cannot be determined experimentally even for the upper part of the glycolytic pathway due to the instability of the mutant TPI [15,16] and some other glycolytic enzymes, HK (hexokinase; EC 2.7.1.1) and PFK (6-phosphofructokinase; EC 2.7.1.11) (results not shown). Therefore, on one hand, we determined the activities of the individual glycolytic enzymes in order to introduce them into the model. On the other hand, we measured the pre-steady-state flux of the subfraction of glycolysis related to the equilibrium of triosephosphates in the haemolysates of the control and the mutant TPI-containing cells.

Activities of the glycolytic enzymes in erythrocytes

Table 2 shows the activities of key glycolytic enzymes in the haemolysates of all family members. Unambiguous increase in the activities of the three glycolytic kinases, HK, PFK and pyruvate kinase (EC 2.7.1.40), was detected in the haemolysates of the two brothers with low TPI activity. This finding revealed that the glycolytic flux could be influenced not only by the decreased TPI activities but by the increased activities of glycolytic kinases as well.

Micropathway analysis

The conversion of FBP into G1,3DP catalysed by aldolase (EC 4.1.2.13), TPI and GAPDH of the haemolysates was measured by monitoring the NAD–NADH conversion at 340 nm. In this micropathway, DHAP and GAP are the intermediates, and the latter is the substrate of the dehydrogenase reaction. Figure 2(A) shows that the rates of the consecutive reactions do not reach the steady state within 60 min (before inactivation of mutant TPI), and that the pre-steady-state flux of the mutant cell is higher than that of the control. The increase of the flux in the haemolysate of the patient is due to the enhanced activities of both aldolase and GAPDH (see Table 2). Figure 2(B) shows that the DHAP concentration reaches virtually a constant level after 100 min in the control, and it continuously increases in time in the case of the mutant enzyme-containing cell, indicating that the mutant TPI is not able to adjust the equilibrium of the triosephosphates. The analysis of this micropathway suggested the potential importance of the enhanced activities of glycolytic enzymes and the lack of rapid equilibrium of triosephosphates in the determination of the overall glycolytic flux.

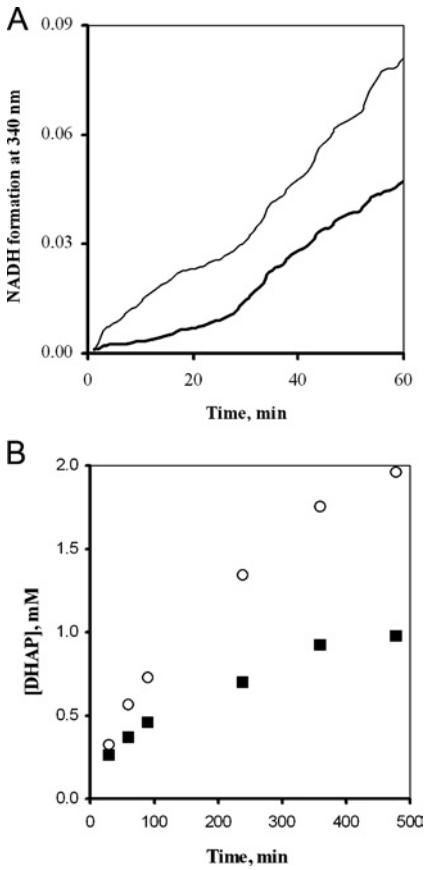

Figure 2 TPI branched pathways: conversion of FBP catalysed by aldolase, TPI and GAPDH

(**A**) Time course of the consecutive reactions. Spectrophotometric measurement was used. NADH formation was monitored at 340 nm. Thick solid line, control; thin solid line, deficient cells. (**B**) Time course of DHAP formation. It was monitored by the two-step determination method. ■, measured values for control; ○, measured values for deficient cells. (**A**, **B**) The haemoglobin content was 1.0 mg/ml (**A**) or 2.5 mg/ml (**B**). Five (**A**) or three (**B**) different sets of experiments were carried out; the S.E.M. for the determinations was ± 10 % (**A**) or ± 15 % (**B**) within each set of experiments.

Realistic model for erythrocyte glycolysis

The mathematical modelling of glycolytic flux does require consideration of changes in the kinetic parameters of the glycolytic enzymes, in addition to that of TPI, to obtain relevant information on the energy state of TPI-deficient erythrocytes. We realized that the mutation-derived activity decrease of TPI was associated with increase in activity of other glycolytic enzymes, including those

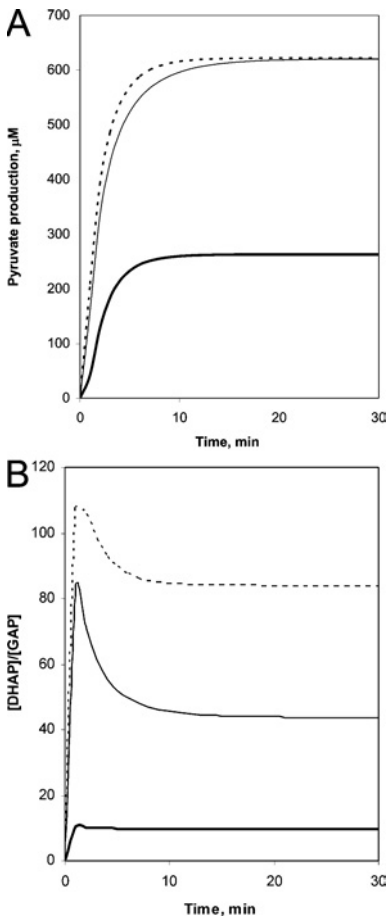

Figure 3 Mathematical modelling of the conversion of glucose into lactate in normal and mutant TPI-containing erythrocytes

(**A**) Time-dependent flux. (**B**) Time-dependent [DHAP]/[GAP] ratio. Thick solid line, model for control; thin solid line, model 1 for patient; dashed line, model 2 for patient.

(HK and PFK) which are known to control predominantly the glycolytic flux in erythrocytes [30–32].

For the modelling of the whole glycolytic pathway, the V_{max} values of the glycolytic enzymes (see Table 2) as well as the K_{equ} (=[DHAP]/[GAP]) and K_m values of the TPI reaction were determined experimentally in the haemolysates from both the control and mutant cells (Supplementary material; see http://www.BiochemJ.org/bj/392/bj3920675add.htm). The rate equations and other kinetic parameters used for computation were taken from Mulquiney and Kuchel [10] and Martinov et al. [9]. The concentrations of glucose, ATP, ADP, pyruvate, lactate, Mg^{2+}, P_i and G2,3DP (2,3-bisphosphoglycerate) were kept constant (see the Materials and methods section). In the case of the patient, models 1 and 2 differ only in the constant ADP and ATP concentrations.

Figure 3(A) shows the time course of the glucose conversion into lactate for the control and the mutant cells. The rate is higher for the mutant cell, and the steady-state flux is increased by a 2.5-fold factor due to the enhanced activities of key enzymes (see Table 2). Then, we tested whether the mathematical model corresponded to the pathological criterion, namely, that the DHAP was accumulated in the haemolysate of the patient. Figure 3(B) shows the computed time course of the DHAP/GAP ratio. In the case of the control, this ratio at the steady state corresponds to the K_{equ} of the TPI reaction as expected; however, it is much higher in the case of the patient. These results show that the mutant TPI is not able to maintain the rapid equilibration between DHAP and GAP. The steady-state concentrations of other metabolites were also computed, and as shown in Table 3, in addition to the concentration of DHAP, the concentration of FBP is increased significantly as well. The alterations in the concentrations of metabolites are related to the new equilibrium adjusted by enzymes with altered activities in the mutant cell. This equilibrium, however, differs from that obtained in normal cells having lower TPI and higher aldolase and GAPDH activities. This new information is assessed by both our experimental data and the mathematical model. The TPI mutation-derived alterations of key glycolytic enzymes represent a 'repairing mechanism' that can ensure a virtually normal energy state in erythrocytes. Indeed, similar ATP levels were found in control and mutant erythrocytes in the case of the Hungarian patient [15].

Searching for differences between the two brothers at the mRNA level

Since the kinetic analysis suggested that the low TPI activity does not result in decreased metabolic flux, we searched for other factors that might be involved in the development of neurodegenerative symptoms in the patient. In DNA microarray experiments for searching for differences between the two brothers

Table 3 Steady-state metabolite concentrations in erythrocytes evaluated from the mathematical model

The concentrations of glucose, ATP, ADP, pyruvate, lactate, Mg^{2+}, P_i and G2,3DP were kept constant at 5, 3, 0.3, 0.06, 1.2, 0.3, 1 and 4.5 mM respectively. In model 2, different ADP value was used for the patient (0.6 mM instead of 0.3 mM, while the sum of ADP and ATP was the same). Reference values give the minimal/maximal values of the normal range. While the average haemoglobin content of blood is approx. 9–11 g/dl for the control with a haematocrit of 0.3, all calculations were done at 300 g/l haemoglobin content. The same haemoglobin value was used for the patient. F6P, fructose-6-phosphate; G6P, glucose-6-phosphate; PEP, phosphoenolpyruvate; 2PG and 3PG, 2- and 3-phosphoglycerate.

	Concentration (μM)				
Metabolite	Reference values	Model for control	Measured for patient	Model 1 for patient	Model 2 for patient
G6P	20–110	91.1	–	72.3	72.3
F6P	6–16	28.2	–	19.9	20.1
FBP	2–30	5.23	70 ± 10	171	79.4
DHAP	7.6–35	19.0	720 ± 90	266	222
GAP	4.8–20	1.94	–	6.09	2.65
DHAP/GAP	–	9.79	–	43.7	83.8
G1,3DP	0.4	1.03	–	2.74	0.91
3PG	55–69	336	–	887	643
2PG	5.5–12	51.6	–	121	87.2
PEP	12–18	72.8	–	95.9	53.3

Table 4 Different mRNA levels between the patient and his brother by microarray experiment

NFAT, nuclear factor of activated T-cells; TNFα, tumour necrosis factor α.

Patient/brother ratio	Gene product	NCBI accession no.
	Repression	
0.42	Erythroid differentiation and denucleation factor 1	AF048849
0.38	Thyroid receptor interacting protein 15	AA496247
0.47	Hybrid receptor gp250	U60975
0.47	Aldehyde dehydrogenase homologue	AI056058
0.47	Transcription factor 14, hepatic nuclear factor	Z49825
	Overexpression	
8.33	Nitric oxide synthase 3 (endothelial cell)	M93718
7.69	POP	X74496
3.57	Retrovirus-related protease homologue	AA923278
3.57	Putative transcriptional repressor E2F-6	AF041381
3.13	Transcription factor NFATx	L41067
2.70	Androgen receptor	M23263
2.70	Interferon γ receptor 1	AA281497
2.27	Solute carrier family 7 (cationic amino acid transporter), member 6	AA418224
2.22	TNF-α converting enzyme	U92649
2.13	NFAT, cytoplasmic 3	H59048

Table 5 Relative mRNA abundance of selected genes in members of the TPI-deficient family by QRT–PCR

For all determinations, at least three independent sets of experiments were carried out. The means $\pm$ S.D. are shown.

	Relative mRNA level			
Gene product	Mother	Father	Brother	Patient
TPI-2	2.24 ± 0.92	0.95 ± 0.31	0.98 ± 0.11	2.24 ± 0.83
TPI-4	1.46 ± 0.82	0.90 ± 0.21	0.92 ± 0.64	1.83 ± 1.25
TPI-7	1.59 ± 0.54	0.87 ± 0.47	0.85 ± 0.41	1.79 ± 0.98

at the mRNA level, 3200 genes were monitored. On the basis of these data, several genes were identified to be repressed or overexpressed in the affected brother compared with those of the healthy brother (Table 4). One of the highest differences (overexpression) was found in POP, the involvement of which was suggested in neurodegenerative processes [33]. QRT–PCR analysis of this protease, in addition to that of TPI, was carried out.

Table 5 shows the mRNA abundance of TPI obtained by QRT–PCR measurements. Unanimously high expression levels of TPI could be detected in the mother and the patient, compared with those obtained in normal individuals, in the father and in the healthy brother, by analysing the N-terminal region (second exon: TPI-2) (Table 5). The larger amount of mRNA determined in the mother and in the patient was confirmed with other probes: i.e. with those of the middle region and the 3′-end (see Table 6). Additional QRT–PCR experiments showed that the mRNA levels of HK, PFK and aldolase do not differ significantly from the control (results not shown).

The increase of TPI mRNA levels in the lymphocytes of the affected brother and the mother did not result in enhancement at the enzyme level. The Western-blot data obtained in the lymphocytes of all family members are shown in Table 1. The larger amounts of mRNA did not result in larger amounts of protein in these two family members; the full-length (wild-type and mutant) TPI levels correspond to that of the control taking into account the

Table 6 Oligonucleotides used in QRT–PCR

The forward primer of TPI-2 and TPI-4 can be found in the second and fourth exons; the corresponding amino acids are VVCAPPT (40–46) and LIGGKV (108–113) respectively. The forward primer of TPI-7 can be found in the last exon, after the coding part of it.

Gene product	Forward primer	Reverse primer
TPI-2	TGGTTTGTGCTCCCCCTACT	CACAGCAATCTTGGGATCTAGCT
TPI-4	GAGCTGATTGGGCAGAAAGTG	CCCAATGCAGGCGATTACTC
TPI-7	AAGCCCAGTAACTGCCCTTTC	ACAGGGTGAAGATATAAACAGTAAAGGAA
β-Actin	TCACCGAGCGCGGCT	TAATGTCACGCACGATTTCCC

Table 7 mRNA levels and activities of POP in the lymphocytes of members of the Hungarian family

The mRNA number of POP was measured by QRT–PCR. The means for three measurements are shown.

		POP activity [nmol of substrate hydrolysed $\cdot$ h^{-1} $\cdot$ (g of protein)$^{-1}$]	
	mRNA number of POP	2.1 μg/ml substrate	0.15 μg/ml substrate
Control	20 ± 5	25.8	1.45
Mother	20 ± 4	31.7	2.02
Brother	22 ± 4	23.6	1.14
Patient	30 ± 6	21.2	0.865

allele compositions. The enzyme activities correlate well with the enzyme levels in the lymphocytes of all family members (note that the full-length mutant TPI carries 30 % relative activity and the activity is lacking in the truncated fragment). It is important to note that the relative activities of TPI in lymphocytes of the two brothers are 10-fold higher than those measured in erythrocytes. Our modelling data suggest that this TPI activity in lymphocytes is virtually enough to adjust the rapid equilibration of the triosephosphates and prevents the accumulation of DHAP as measured experimentally as well (results not shown).

Table 7 shows the mRNA abundance and enzyme activity of POP in lymphocytes of the Hungarian family members. Increased mRNA level was observed only in the lymphocytes of the affected brother. The enzyme activity was, however, not increased. The lowest value was measured in the sample of the affected brother. Significantly lower activity was obvious in the case of the patient at subsaturation concentration of substrate. Thus the decreased activity of POP would be indicative of an effect on K_m. The extent of decrease ($\sim$30 %) is similar to that found in post-mortem brain tissues of patients with Alzheimer's disease, Parkinson's disease or Huntington's disease [33]. In contrast with this, the activity of POP was normal in the lymphocytes of the neurologically intact brother.

DISCUSSION

Many glycolytic enzymopathies were found in erythrocytes [3]. In most of these studies, the activities of the mutant enzymes were determined without examining the consequences of the mutation at metabolic levels. In other studies, the effect of mutations was investigated at the system level by computer models by including the activity of the mutant enzyme, but the possibility of changes in the activity of other glycolytic enzymes was not considered [8,9].

We have found that the steady-state rate of glycolysis cannot be measured under the conditions used because of the loss of

enzymatic activity of the mutant TPI. However, correct values for kinetic parameters of the individual enzymes can be obtained from the initial rates, when virtually no enzyme inactivation occurs, and then the glycolytic flux can be computed. By introducing the relevant kinetic parameters (the enhanced activities of the glycolytic kinases, aldolase and GAPDH) and rate equations, we evaluated a realistic mathematical model with the accumulation of DHAP in the mutant cell. In addition to the accumulation of DHAP, our model has shown that FBP level is also increased due to the TPI mutation (Table 3). This is because the aldolase-catalysed reaction is highly reversible and thus the high DHAP level renders possible the maintenance of a non-physiological FBP level.

Schuster and Holzhütter [8] presented earlier a model where approx. 0.1 % TPI activity was suggested to be enough to provide a normal DHAP level. We suggest that the changes in metabolite concentration may not be due to a decreased TPI activity alone but changes in activity of other glycolytic enzymes may be implicated.

Another important finding evaluated from our modelling studies is the lack of reduction of the glycolytic rate in the deficient cell. This is mainly due to the activation of glycolytic kinases. These kinases were likely to be activated since virtually no increase in their mRNA levels was detected (results not shown). Nevertheless, an increase in the expression of these enzymes cannot be excluded. All these effects result in a glycolytic flux maintaining the physiological ATP level in the cells of the patient [15].

TPI-deficient patients suffering from haemolytic anaemia were suspected to have reticulocytosis, which generally has higher enzyme activities and, therefore, the activity of a given enzyme determined in the erythrocyte population is often overestimated [7]. However, we can exclude this possibility, because the brothers have only slightly increased reticulocyte counts (3 % versus 1 %) [13]; and certain enzymes, e.g. lactate dehydrogenase (EC 1.1.1.27) and enolase (EC 4.2.1.11), have the same activities in the control and deficient cells (see Table 2).

In lymphocytes, a significantly higher mRNA level was detected for TPI of the mother and the affected brother; however, this difference disappeared at the enzyme level, and the TPI activities of the two brothers were similar and virtually high enough to adjust the rapid equilibration of the triosephosphates. The altered gene expression of TPI seems to confirm our previous assumption, based on the similarities found in the patient and his mother, i.e. the presence of an additional inherited genetic or epigenetic factor [16]. It has to be, however, taken into account that recent publications (for instance, that of Morley et al. [34]) have revealed that natural variation in gene expression is extensive in humans and other organisms, variation in baseline expression level of many genes has a heritable component and that expression levels of many genes that share the same regulatory region are significantly correlated.

In the search for other factor(s) involved in the development of the neurological disorder, we have found a large difference in eNOS (endothelial nitric oxide synthase; EC 1.14.13.39) and POP mRNA levels of the two brothers. eNOS increases the production of nitric oxide responsible for the nitration of tyrosine residues. Previously, we reported a 15-fold increase in the urinary 3-nitrotyrosine of the patient compared with that of the control or the healthy brother [35]. Interestingly, TPI has been recently identified as one of the main proteins nitrotyrosinated by eNOS in the case of Alzheimer's disease [36]. The POP activity in the cells of the patient was reduced by 40 and 30 % with respect to the control and the healthy brother respectively. POP is ubiquitously distributed in various tissues and cell types. It plays a key role in the general intracellular protein degradation processes [33], in neurotransmission, in activation of cell-mediated immunity and in cellular response to heat shock [37]. There are a few reports suggesting that the reduction of POP activity in brain tissues may contribute to the development of the neurodegenerative process in Alzheimer's, Parkinson's and Huntington's diseases [33].

Similar to other neurodegenerative diseases, the relationship of the mutant protein (TPI, β-amyloid, huntingtin etc.) and activity of POP is unclear as yet. It is a new observation that decreased POP activity was detected in the blood cells of a patient with neurodegenerative symptoms.

The decrease in POP activity may be an early response to cellular stress as suggested by Mantle et al. [33]. The oxidative stress associated with hypoxia was found to be accompanied by an increase in the TPI protein level [38]. This is consistent with an up-regulation of TPI to compensate for its loss of activity by oxidative modification. We have revealed imbalance in the pro-oxidant/antioxidant homoeostasis as well as an increased rate of methylglyoxal and protein glycation, oxidation and nitrosation in our TPI-deficient patient. All these changes are known to be important factors in the mechanism of neurodegeneration [35,39].

The excellent technical contribution of Ilona Szamosi (Institute of Enzymology, Budapest, Hungary) is gratefully acknowledged. This work was supported by grants from the Hungarian National Science Foundation OTKA (T-033138 to S. H., T-035019 and T-049247 to F. O. and T-046071 and B-044730 to Judit Ovádi), from the Hungarian Medical Research Council (ETT-408 to S. H.), from the Hungarian Ministry of Education (OMFB-00701/2003 to Judit Ovádi and OMFB-00702/2003 to S. H.), FP6-2003-LIFESCIHEALTH-I: Bio-Sim, NKFP-MediChem2 1/A/005/2004, and by Charles Simonyi fellowship (to Judit Ovádi).

REFERENCES

1 Mande, S. C., Mainfroid, V., Kalk, K. H., Goraj, K., Martial, J. A. and Hol, W. G. J. (1994) Crystal structure of recombinant human triosephosphate isomerase at 2.8A resolution. Triosephosphate isomerase-related human genetic disorders and comparison with the trypanosomal enzyme. Protein Sci. **3**, 810–821

2 Albery, W. J. and Knowles, J. R. (1977) Efficiency and evolution of enzyme catalysis. Angew. Chem. Int. Ed. Engl. **16**, 285–293

3 Valentine, W. N. and Paglia, D. E. (1984) Erythrocyte enzymopathies, hemolytic anemia, and mutisystem disease: an annotated review. Blood **64**, 583–591

4 Schneider, A. S. (2000) Triosephosphate isomerase deficiency: historical perspectives and molecular aspects. Baillieres Best Pract. Res. Clin. Haematol. **13**, 119–140

5 Eber, S. W., Pekrun, A., Bardosi, A., Gahr, M., Krietsch, W. K., Kruger, J., Matthei, R. and Schroter, W. (1991) Triosephosphate isomerase deficiency: haemolytic anaemia, myopathy with altered mitochondria and mental retardation due to a new variant with accelerated enzyme catabolism and diminished specific activity. Eur. J. Pediatr. **150**, 761–766

6 Rosa, R., Prehu, M. O., Calvin, M. C., Badoual, J., Alix, D. and Girod, R. (1985) Hereditary triosephosphate isomerase deficiency: seven new homozygous cases. Hum. Genet. **71**, 235–240

7 Zanella, A., Mariani, M., Colombo, M. B., Borgna-Pignatti, C., de Stefano, P., Morgese, G. and Sirchia, G. (1985) Triosephosphate isomerase deficiency: 2 new cases. Scand. J. Haematol. **34**, 417–424

8 Schuster, R. and Holzhütter, H. G. (1995) Use of mathematical models for predicting the metabolic effect of large-scale enzyme activity alterations. Application to enzyme deficiencies of red blood cells. Eur. J. Biochem. **229**, 403–418

9 Martinov, M. V., Plotnikov, A. G., Vitvitsky, V. M. and Ataullakhanov, F. I. (2000) Deficiencies of glycolytic enzymes as a possible cause of hemolytic anemia. Biochim. Biophys. Acta **1474**, 75–87

10 Mulquiney, P. J. and Kuchel, P. W. (1999) Model of 2,3-bisphosphoglycerate metabolism in the human erythrocyte based on detailed enzyme kinetic equations: equations and parameter refinement. Biochem. J. **342**, 581–596

11 Tanaka, K. R. and Zerez, C. R. (1990) Red cell enzymopathies of the glycolytic pathway. Semin. Hematol. **27**, 165–185

12 Orosz, F., Wágner, G., Liliom, K., Kovács, J., Baróti, K., Horányi, M., Farkas, T., Hollán, S. and Ovádi, J. (2000) Enhanced association of mutant triosephosphate isomerase to red cell membranes and to brain microtubules. Proc. Natl. Acad. Sci. U.S.A. **97**, 1026–1031

13 Chang, M.-L., Artymiuk, P. J., Wu, X., Hollán, S., Lammi, A. and Maquat, L. E. (1993) Human triosephosphate isomarese deficiency resulting from mutation of Phe-240. Am. J. Hum. Genet. **52**, 1260–1269
14 Valentin, C., Cohen-Solal, M., Maquat, L. E., Horányi, M., Inselt-Kovács, M. and Hollán, S. (2000) Identical germ-line mutations in the triosephosphate isomerase alleles of two brothers associated with distinct clinical phenotypes. C.R. Acad. Sci. III **323**, 245–250
15 Hollán, S., Fujii, H., Hirono, A., Hirono, K., Karro, H., Miwa, S., Harsanyi, V., Gyodi, E. and Inselt-kovács, M. (1993) Hereditary triosephosphate isomerase (TPI) deficiency: two severely affected brothers one with and one without neurological symptoms. Hum. Genet. **92**, 486–490
16 Orosz, F., Oláh, J., Alvarez, M., Keserü, G. M., Szabó, B., Wágner, G., Kovári, Z., Horányi, M., Baróti, K., Martial, J. A. et al. (2001) Distinct behavior of mutant triosephosphate isomerase in hemolysate and in isolated form: molecular basis of enzyme deficiency. Blood **98**, 3106–3112
17 Oláh, J., Orosz, F., Keserü, G. M., Kovári, Z., Kovács, J., Hollán, S. and Ovádi, J. (2002) Triosephosphate isomerase deficiency: a neurodegenerative misfolding disease. Biochem. Soc. Trans. **30**, 30–38
18 O'Dorisio, M. S. and Panerai, A. (eds) (1990) Neuropeptides and immunopeptides: messengers in a neuroimmune axis. Ann. N.Y. Acad. Sci. **594**, 1–361
19 Onody, A., Zvara, A., Hackler, Jr, L., Vigh, L., Ferdinandy, P. and Puskas, L. G. (2003) Effect of classic preconditioning on the gene expression pattern of rat hearts: a DNA microarray study. FEBS Lett. **536**, 35–40
20 Pfaffl, M. W. (2001) A new mathematical model for relative quantification in real-time RT-PCR. Nucleic Acids Res. **29**, e45
21 Puskás, L. G., Hackler, Jr, L., Kovács, G., Kupihar, Z., Zvara, A., Micsik, T. and van Hummelen, P. (2002) Recovery of cyanine-dye nucleotide triphosphates. Anal. Biochem. **305**, 279–281
22 Palotás, A., Puskás, L. G., Kitajka, K., Palotás, M., Molnár, J., Pakaski, M., Janka, Z., Penke, B. and Kalman, J. (2004) The effect of citalopram on gene expression profile of Alzheimer lymphocytes. Neurochem. Res. **29**, 1563–1570
23 Puskas, L. G., Zvara, A., Hackler, Jr, L., Micsik, T. and van Hummelen, P. (2002) Production of bulk amounts of universal RNA for DNA microarrays. Biotechniques **33**, 898–900, 902, 904
24 Cleveland, W. S. (1974) Robust locally weighted regression and smoothing scatterplots. J. Am. Stat. Assoc. **74**, 829–836
25 Yang, Y. H., Dudoit, S., Luu, P., Lin, D. M., Peng, V., Ngai, J. and Speed, T. P. (2002) Normalization for cDNA microarray data: a robust composite method addressing single and multiple slide systematic variation. Nucleic Acids Res. **30**, e15
26 Bradford, M. M. (1976) A rapid and sensitive method for the quantitation of microgram quantities of protein utilizing the principle of protein-dye binding. Anal. Biochem. **72**, 248–254
27 Minakami, S., Suzuki, C., Saito, T. and Yoshikawa, H. (1965) Studies on erythrocyte glycolysis. I. Determination of the glycolytic intermediates in human erythrocytes. J. Biochem. (Tokyo) **58**, 543–550
28 Beutler, E., Blume, K. G., Kaplan, J. C., Löhr, G. W., Ramot, B. and Valentine, W. N. (1977) International Committee for Standardization in Haematology: recommended methods for red-cell enzyme analysis. Br. J. Haematol. **35**, 331–340
29 Polgár, L. (1994) Prolyl oligopeptidases. Methods Enzymol. **244**, 188–200
29a Orosz, F. and Ovádi, J. (1986) Dynamic interactions of enzymes involved in triosephosphate metabolism. Eur. J. Biochem. **160**, 615–619
30 Rapoport, T. A., Heinrich, R. and Rapoport, S. M. (1976) The regulatory principles of glycolysis in erythrocytes *in vivo* and *in vitro*. A minimal comprehensive model describing steady states, quasi-steady states and time-dependent processes. Biochem. J. **154**, 449–469
31 Kuchel, P. W., Chapman, B. E., Lovric, V. A., Raftos, J. E., Stewart, I. M. and Thorburn, D. R. (1984) The relationship between glucose concentration and rate of lactate production by human erythrocytes in an open perfusion system. Biochim. Biophys. Acta **805**, 191–203
32 Mulquiney, P. J. and Kuchel, P. W. (1999) Model of 2,3-bisphosphoglycerate metabolism in the human erythrocyte based on detailed enzyme kinetic equations: computer simulation and metabolic control analysis. Biochem. J. **342**, 597–604
33 Mantle, D., Falkous, G., Ishiura, S., Blanchard, P. J. and Perry, E. K. (1996) Comparison of proline endopeptidase activity in brain tissue from normal cases and cases with Alzheimer's disease, Lewy body dementia, Parkinson's disease and Huntington's disease. Clin. Chim. Acta **249**, 129–139
34 Morley, M., Molony, C. M., Weber, T. M., Devlin, J. L., Ewens, K. G., Spielman, R. S. and Cheung, V. G. (2004) Genetic analysis of genome-wide variation in human gene expression. Nature (London) **430**, 743–747
35 Ahmed, N., Battah, S., Karachalias, N., Babaei-Jadidi, R., Horányi, M., Baróti, K., Hollán, S. and Thornalley, P. J. (2003) Increased formation of methylglyoxal and protein glycation, oxidation and nitrosation in triosephosphate isomerase deficiency. Biochim. Biophys. Acta **1639**, 121–132
36 Coma, M., Guix, F. X., Uribesalgo, I., Espuna, G., Solé, M., Andreu, D. and Munoz, F. J. (2005) Lack of oestrogen protection in amyloid-mediated endothelial damage due to protein nitrotyrosination. Brain **128**, 1613–1621
37 Gibson, A. M., Edwardson, J. A. and McDermott, J. R. (1991) Post mortem levels of some brain peptidases in Alzheimer's disease: reduction in proline endopeptidase activity in cerebral cortex. Neurosci. Res. Commun. **9**, 73–81
38 Poon, H. F., Castegna, A. and Farr, S. A. (2004) Quantitative proteomics analysis of specific protein expression and oxidative modification in aged senescence-accelerated prone 8 mice brain. Neuroscience **126**, 915–926
39 Karg, E., Németh, I., Horányi, M., Pintér, S., Vécsei, L. and Hollán, S. (2000) Diminished blood levels of reduced glutathione and alpha-tocopherol in two triosephosphate isomerase-deficient brothers. Blood Cells Mol. Dis. **26**, 91–100

Received 22 June 2005/5 August 2005; accepted 9 August 2005
Published as BJ Immediate Publication 9 August 2005, doi:10.1042/BJ20050993